Liquid Crystals
Publication details, including instructions for authors and subscription information:
http://www.informaworld.com/smpp/title~content=t713926090

Columnar and interdigitated structures from apolar discotic mesogens with radial dipoles: a Monte Carlo study

Roberto Berardi[a]; Silvia Orlandi[a]; Claudio Zannoni[a]
[a] Dipartimento di Chimica Fisica e Inorganica, and INSTM, Università, 40136 Bologna, Italy

To cite this Article Berardi, Roberto , Orlandi, Silvia and Zannoni, Claudio(2005) 'Columnar and interdigitated structures from apolar discotic mesogens with radial dipoles: a Monte Carlo study', Liquid Crystals, 32: 11, 1427 — 1436
To link to this Article: DOI: 10.1080/02678290500160696
URL: http://dx.doi.org/10.1080/02678290500160696

Liquid Crystals, Vol. 32, No. 11–12, November–December 2005, 1427–1436

Columnar and interdigitated structures from apolar discotic mesogens with radial dipoles: a Monte Carlo study

ROBERTO BERARDI, SILVIA ORLANDI and CLAUDIO ZANNONI*

Dipartimento di Chimica Fisica e Inorganica, and INSTM, Università, Viale del Risorgimento 4, 40136 Bologna, Italy

(*Received 19 January 2005; accepted 24 March 2005*)

We have simulated, using a Monte Carlo method, a system of apolar Gay–Berne discotic particles without dipoles and with two or three dipoles symmetrically embedded in the disc. The dipoleless system can form nematic and hexagonal columnar mesophases. Adding two in-plane antiparallel radial dipoles has the effect of destabilizing the columnar ordering, in favour of a fully interdigitated arrangement of the molecular stacks, with strong correlations in the plane perpendicular to the director and large biaxiality. No columnar phase is observed for the systems with three planar radial dipoles with threefold symmetry up to very low temperatures. Finally, on decreasing the strength of the three dipoles, a columnar non-interdigitated phase is observed.

1. Introduction

Discotics form an important and rapidly growing family of liquid crystals [1]. The typical structure of a discotic is that of a flat core with a number of chains attached [1, 2]. The central core has been realized with a large variety of aromatic structures, starting in particular from the classic triphenylenes and truxenes, to now include superyines, coronenes, phthalocyanines and a large variety of other moieties [3–5]. This flexibility in the choice of structures allows the possibility of selecting cores and inserting groups that confer on the molecule properties of interest in applications such as charge transfer ability or a suitable charge distribution. One of the most promising applications of columnar systems is in 'molecular wires', where regularity seems to be important in enhancing electron or hole mobility along the column [6]. In order to understand at least some of the general aspects and trends involved, a molecular model, rather than an atomistic one requiring us to address a specific compound, is of use.

One of the simplest possibilities for controlling ordering seems to be that of introducing substituents that endow the molecules with one or more dipole moments [7]. An understanding of the effects on phase organization of these dipole moments is, on the one hand, not obvious, given the complex interplay between the different intermolecular contributions; and, on the other hand, essential from the point of view of a rational molecular design of new discotic materials [8].

Here we have modelled the discotic mesogen using a Gay–Berne (GB) [9–11] attractive–repulsive potential, without dipoles and with a set of two or three embedded dipoles located at selected positions in the molecular plane, to examine their overall molecular and dipolar organization. We have employed Monte Carlo (MC) 'experiments' to investigate several temperatures corresponding to nematic and columnar liquid crystal phases in the isobaric–isothermal (NPT) ensemble, paying attention to the characterization of the low temperature phase, which is found to be particularly sensitive to the dipolar configuration.

2. The model

We have considered uniaxial oblate particles with axes σ_e and σ_s ($\sigma_e<\sigma_s$) without dipoles, and with n=2, 3 embedded lateral planar electric point dipoles placed off centre [12], so as to give D_{nh} symmetry, as shown in figure 1; positions and orientations of dipoles are given in table 1.

The pair potential is the sum of a Gay–Berne and a dipole–dipole term: $U^*_{ij}\equiv U_{ij}\big/\epsilon_s=U^{GB*}_{ij}+U^{d*}_{ij}$. The Gay–Berne term has a repulsive and attractive contribution with a 12–6 inverse distance dependence form

$$U^{GB*}_{ij}=4\epsilon(\hat{\mathbf{z}}_i,\hat{\mathbf{z}}_j,\hat{\mathbf{r}})\times\left[\left\{\frac{\sigma_e}{r-\sigma(\hat{\mathbf{z}}_i,\hat{\mathbf{z}}_j,\hat{\mathbf{r}})+\sigma_e}\right\}^{12}-\left\{\frac{\sigma_e}{r-\sigma(\hat{\mathbf{z}}_i,\hat{\mathbf{z}}_j,\hat{\mathbf{r}})+\sigma_e}\right\}^{6}\right] \quad (1)$$

*Corresponding author. Email: Claudio.Zannoni@cineca.it

Liquid Crystals
ISSN 0267-8292 print/ISSN 1366-5855 online © 2005 Taylor & Francis
http://www.tandf.co.uk/journals
DOI: 10.1080/02678290500160696

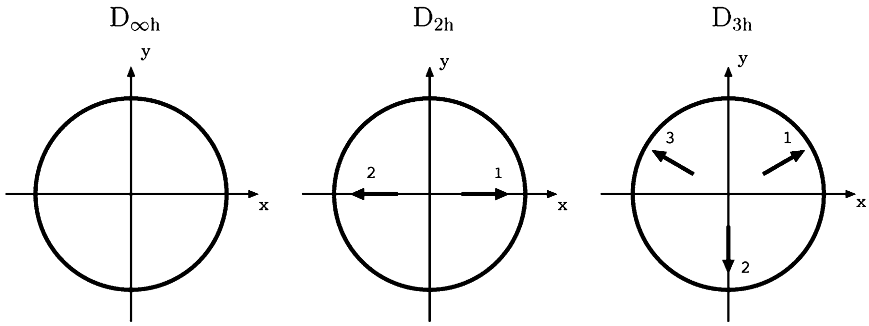

Figure 1. A sketch of the D_{nh} molecular model employed, showing position and orientation of the permanent dipoles.

Table 1. Position and orientation of dipoles in the D_{2h} and D_{3h} model discotic particles.

Symmetry	Dipole	α	β	r_x	r_y	r_z
D_{2h}	1	0	90°	$\sigma_s/4$	0	0
	2	0	270°	$-\sigma_s/4$	0	0
D_{3h}	1	0	60°	$\sqrt{3}/8\sigma_s$	$\sigma_s/8$	0
	2	0	180°	0	$-\sigma_s/4$	0
	3	0	300°	$-\sqrt{3}/8\sigma_s$	$\sigma_s/8$	0

with unit vectors $\hat{z}_i, \hat{z}_j$ defining the orientation of the principal axes of particles i and j taken along their symmetry axes, while $r = r_j - r_i \equiv r\hat{r}$ is the intermolecular vector of length r.

Since here we are dealing with general trends, we employ the parameterization used in [12, 13] based on the dimensions of a triphenylene core, namely: shape anisotropy $\sigma_e/\sigma_s = 0.345$, interaction anisotropy $\epsilon_e/\epsilon_s = 5$, and using GB parameters $\mu = 1$ and $\nu = 3$. The coefficients σ_s and ϵ_s are used as molecular units of length and energy. The cutoff radius adopted is $r_c = 1.4\sigma_s$. We have shown elsewhere that this discotic GB system, with a single axial [12] and transverse [13] dipole, yields a discotic nematic and hexagonal columnar phase. The pair dipolar energy term is given by

$$U_{ij}^{d*} = \frac{\mu_i^* \mu_j^*}{r^3}\left[\hat{\boldsymbol{\mu}}_i \cdot \hat{\boldsymbol{\mu}}_j - 3\left(\hat{\boldsymbol{\mu}}_i \cdot \hat{\mathbf{r}}\right)\left(\hat{\boldsymbol{\mu}}_j \cdot \hat{\mathbf{r}}\right)\right]. \quad (2)$$

Here, we have used reduced dipole moments $\mu^* = \left(\mu^2/\epsilon_s\sigma_s^3\right)^{1/2} = 0.6$ and $\mu^* = 0.4$ which, when considering for instance a molecular diameter of $\sigma_s \approx 10$ Å, and an energy term $\epsilon_s = 5 \times 10^{-15}$ erg, correspond to about 1.2 D and 0.8 D. The electrostatic energy has been evaluated using the reaction field method [14] with reaction field radius $r_{RF} = 3\sigma_s$ and with a dielectric continuum permittivity $\epsilon_{RF} = 1.5$. This was shown to be adequate in comparison with the more rigorous Ewald summation for this type of system as shown in previous works [15–17].

Simulations were run in the isobaric–isothermal (NPT) ensemble (constant number of molecules $N = 1000$, dimensionless pressure $P^* \equiv P\sigma_s^3/\epsilon_s = 5$ and dimensionless temperature $T^* \equiv k_B T/\epsilon_s$), using periodic boundary conditions. All MC runs were started from well equilibrated isotropic configurations of the dipoleless system and a cubic box, and were run in a cooling sequence with equilibration runs of ≈300 kcycles, where a cycle corresponds to N attempted MC moves. The box shape was adjusted during volume update moves in order to avoid the formation of holes. Box edges were allowed to vary in length independently, but kept mutually orthogonal.

3. Results and discussion

We have determined from the simulations some useful physical quantities: average energies $\langle U^{GB*} \rangle$, $\langle U^{d*} \rangle$, and orientational order parameters [18], i.e.

$$\langle R_{00}^2 \rangle = \langle P_2 \rangle = \langle \left(3\cos^2\beta - 1\right)/2 \rangle \quad (3)$$

and

$$\langle R_{22}^2 \rangle = \langle \left(1 + \cos^2\beta\right)\cos 2\alpha \cos 2\gamma/4 - \cos\beta \sin 2\alpha \sin 2\gamma/2 \rangle \quad (4)$$

where α, β and γ are the Euler angles giving the orientation of the molecular axis system ($\hat{\mathbf{x}}, \hat{\mathbf{y}}, \hat{\mathbf{z}}$) in the director frame ($\hat{\mathbf{X}}, \hat{\mathbf{Y}}, \hat{\mathbf{Z}}$).

Phase structure was characterized through the radial distribution function

$$g_0(r) = 1/\left(4\pi r^2 \rho\right)\langle \delta\left(r - r_{ij}\right) \rangle_{ij} \quad (5)$$

and its second rank anisotropy

$$g_2^+(r) = \langle \delta\left(r - r_{ij}\right) P_2\left(\cos\beta_{ij}\right) \rangle_{ij} \quad (6)$$

where β_{ij} is the angle between the intermolecular vector $\mathbf{r}_{ij}$ and the phase director $\hat{\mathbf{Z}}$ [19], and the average $\langle \ldots \rangle_{ij}$ is computed over all molecular pairs.

We now briefly comment on each of the various systems studied.

3.1. *Dipole-less* ($D_{\infty h}$)

Starting from the highest temperature studied $T^*=8.0$, the first observation is that the system is isotropic. As the temperature is reduced, orientational order develops and the molecules organize in a nematic and then, by further lowering T^*, in a columnar hexagonal phase. Snapshots of the molecular organizations, at T^* corresponding to the columnar phase, are shown in figure 2, where we have colour coded the orientations of the molecules relative to the phase director, in order to highlight their orientational ordering.

We plot in figure 3 the temperature dependence of the average energy per particle, and uniaxial and biaxial order parameters for the systems studied, while numerical values of the observables and phase assignments are reported in table 2, given in the Appendix. The order parameter $\langle R^2_{00}\rangle$ increases sharply when the nematic is formed, at $T^*=6.4$, and grows regularly with no significant jumps when the columnar phase is formed. The biaxial $\langle R^2_{22}\rangle$ parameter is zero within error at all temperatures and is shown as a check.

The $g_0(r)$, figure 4(*a*), presents, for the low temperature columnar phase ($T^*=4.0$), several well defined peaks related to the detailed structure of this mesophase. In particular, the first two maxima at $r^*=0.35$, 0.7 correspond to the first two neighbouring pairs within the same column. The next two maxima are due to adjacent pairs of molecules belonging to different columns and their position indicates a hexagonal

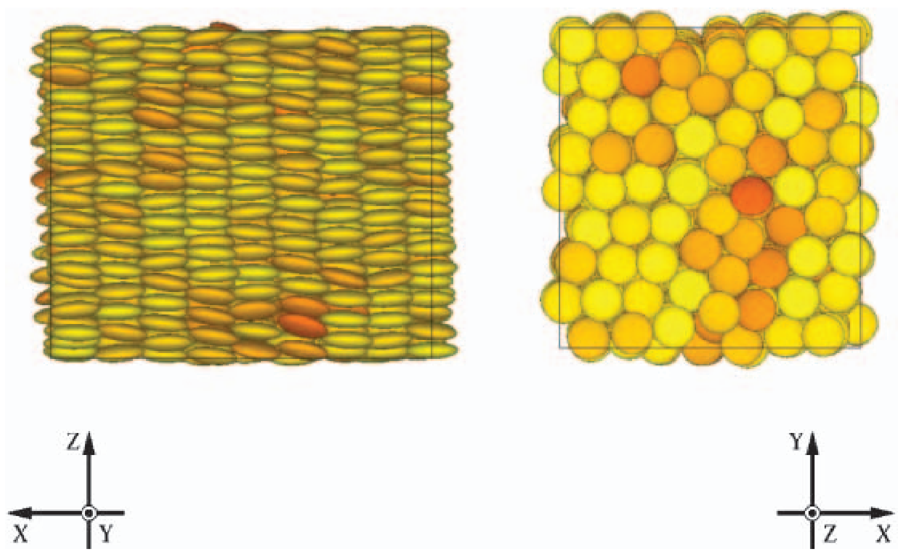

Figure 2. Snapshots of MC–NPT configurations (side and top views) of systems of $N=1000$ dipole-less GB discs at $P^*=100$ and temperatures $T^*=4.0$ (phase C_h). The orientation of the director frame is also shown.

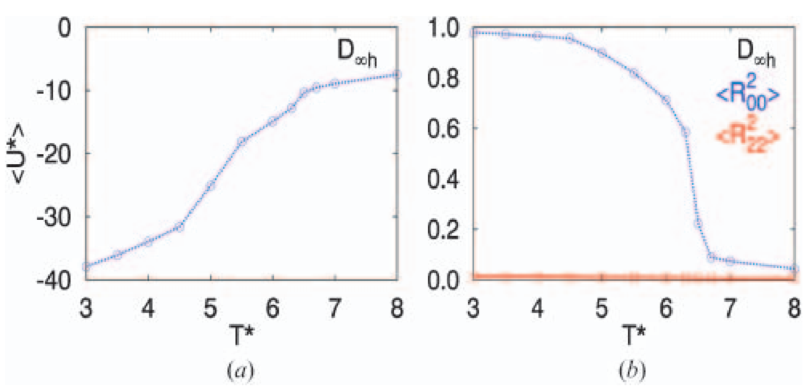

Figure 3. (*a*) Average total energy per particle $\langle U^*_{ij}\rangle$, (*b*) orientational and biaxial order parameters $\langle R^2_{00}\rangle$ and $\langle R^2_{22}\rangle$ for a system of $N=1000$ dipole-less GB discs at $P^*=100$ as a function of temperature T^*.

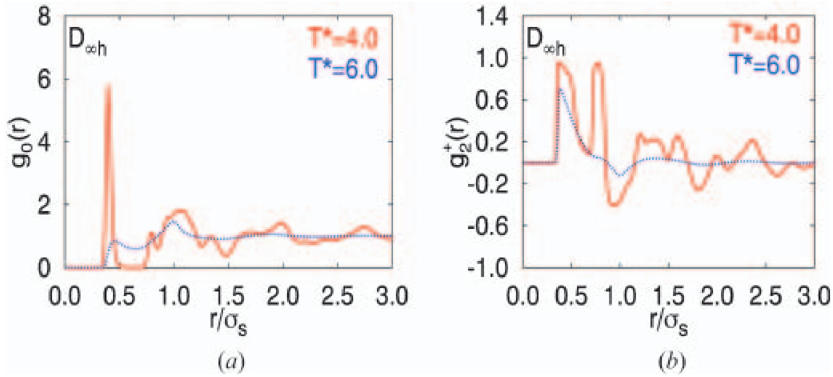

Figure 4. (*a*) Radial correlation function $g_0(r)$, (*b*) second rank anisotropy $g_2^{+}(r)$ for systems of $N=1000$ dipole-less GB discs at $P^*=100$ and temperatures $T^*=4.0$ (phase C_h) and 6.0 (phase N).

arrangement of interdigitated columns. An increase in temperature ($T^*=6.0$) gives a nematic phase and the radial correlation function shows no positional ordering: side-by-side configurations are approximately as probable as face-to-face.

Further details on the phase structure can be obtained by studying the second rank anisotropy $g_2^{+}(r)$, see figure 4(*b*). In correspondence to the columnar phases the anisotropy exhibits a detailed structure even for high molecular separations, showing two positive maxima for the intracolumn neighbouring pairs (intermolecular vector parallel to the director) and a third negative peak corresponding to molecules belonging to adjacent columns (intermolecular vector perpendicular to the director).

3.2. *Two dipoles (D_{2h})*

The introduction of two antiparallel dipoles has quite a pronounced effect on the phase behaviour. Examining the order first, see figure 5(*b*), we see that the transition from the isotropic to a uniaxially ordered system ($\langle R_{00}^2\rangle \neq 0$, $\langle R_{22}^2\rangle = 0$) is still taking place roughly in the same temperature region ($T^*\approx 6$) as for the dipoleless system. Moreover at $T^*\approx 5$ a new, strongly biaxial, molecular organization sets in. Correspondingly to the biaxial ordering $\langle R_{22}^2\rangle > 0$, the energy shows a significant stabilization due to the electrostatic energy (see figure 5(*a*)). It is immediately clear that the structure is quite different from the standard columnar organization by a comparison of the radial distributions $g_0(r)$ and $g_2^{+}(r)$ shown in figure 6. We note that even if the structure seems more disordered, some positional ordering of the phase still exists as shown by the $g_0(r)$ peaks.

The nature of the phase organization becomes clear when observing typical snapshots from the simulation in the biaxial region (figure 7) that indicate a regular intercalated structure with local pairing of dipoles from neighbouring molecules. This effective dipole locking explains the electrostatic energy contribution increase, figure 5(*a*). The observed interdigitation is highly directional in the direction perpendicular to the director. We note that although the two antiparallel dipoles imply a non-vanishing molecular quadrupole,

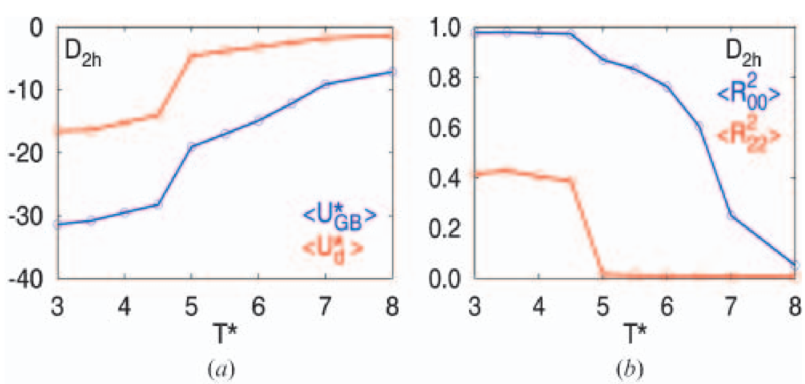

Figure 5. (*a*) Average GB and dipolar energy contributions $\langle U_{ij}^{GB*}\rangle$ and $\langle U_{ij}^{d*}\rangle$, (*b*) orientational and biaxial order parameters $\langle R_{00}^2\rangle$ and $\langle R_{22}^2\rangle$ for a system of $N=1000$ GB discs with two planar dipoles at $P^*=100$ as a function of temperature T^*.

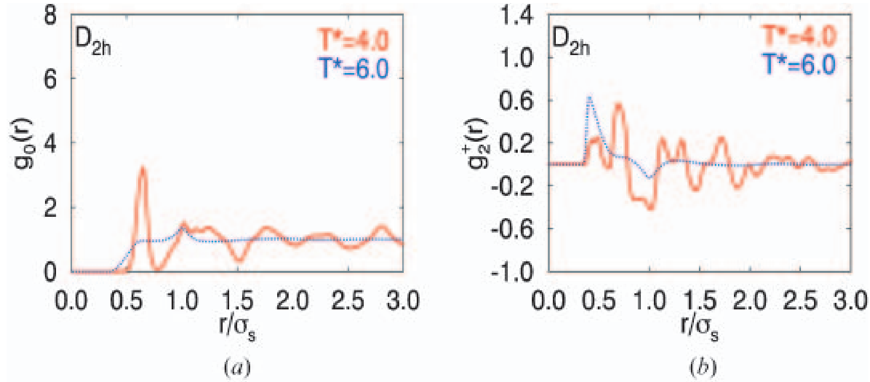

Figure 6. (*a*) Radial correlation function $g_0(r)$, (*b*) second rank anisotropy $g_2^{+}(r)$ for systems of $N=1000$ GB discs with two planar dipoles at $P^*=100$ and temperatures $T^*=4.0$ (phase N_{bx}), and 6.0 (phase N).

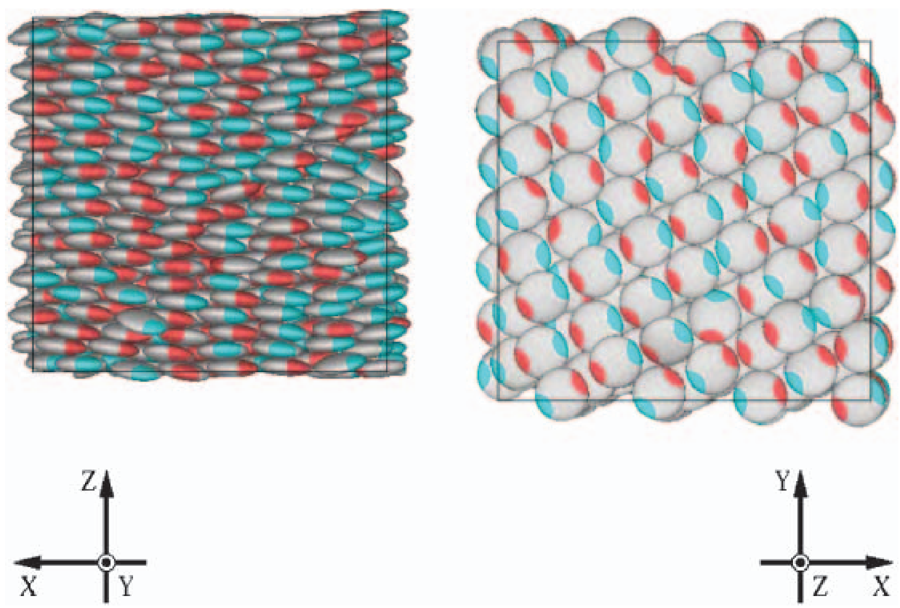

Figure 7. Snapshots of MC–NPT configurations (side and top views) of systems of $N=1000$ GB discs with two planar dipoles at $P^*=100$ and temperature $T^*=4.0$ (phase N_{bx}). The red and cyan 'patches' label the molecular dipoles, and the director frame is also shown.

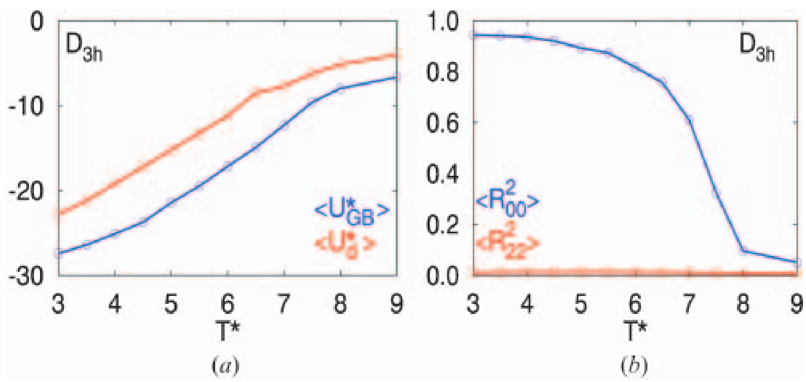

Figure 8. (*a*) Average GB and dipolar energy contributions $\langle U_{ij}^{GB*}\rangle$ and $\langle U_{ij}^{d*}\rangle$, and (*b*) orientational and biaxial order parameters $\langle R_{00}^2\rangle$ and $\langle R_{22}^2\rangle$ for a system of $N=1000$ GB discs with three planar dipoles $\mu^*=0.6$ at $P^*=100$ as a function of temperature T^*.

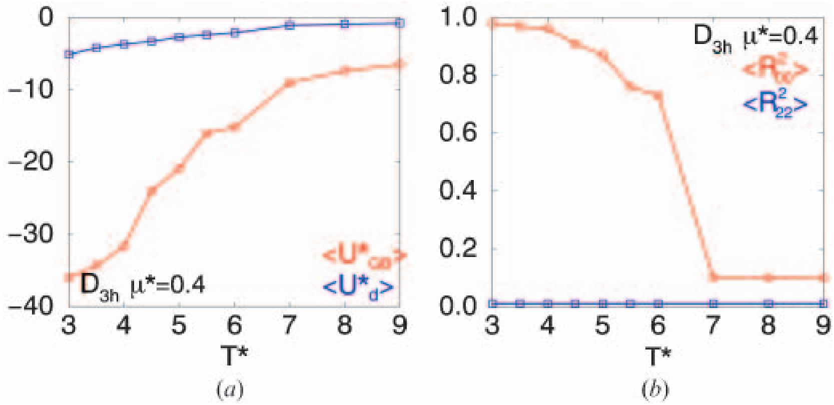

Figure 9. (*a*) Average GB and dipolar energy contributions $\langle U_{ij}^{GB*} \rangle$ and $\langle U_{ij}^{d*} \rangle$, and (*b*) orientational and biaxial order parameters $\langle R_{00}^2 \rangle$ and $\langle R_{22}^2 \rangle$ for a system of $N=1000$ GB discs with three planar dipoles $\mu^*=0.4$ at $P^*=100$ as a function of temperature T^*.

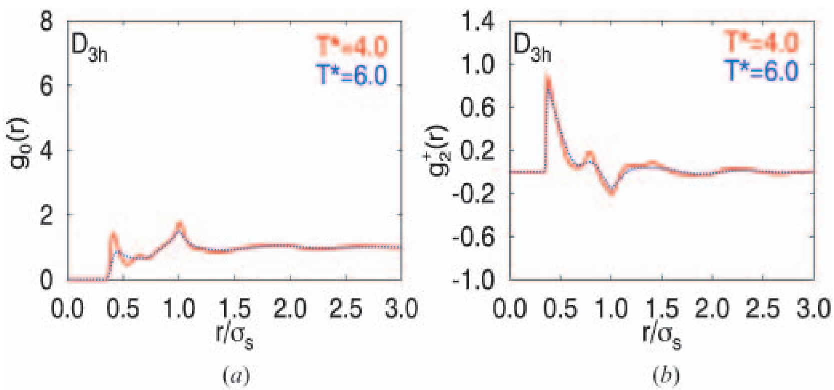

Figure 10. (*a*) Radial correlation function $g_0(r)$, (*b*) second rank anisotropy $g_2^+(r)$ for systems of $N=1000$ GB discs with three planar dipoles $\mu^*=0.6$ at $P^*=100$ and temperatures $T^*=4.0$ (phase N) and 6.0 (phase N).

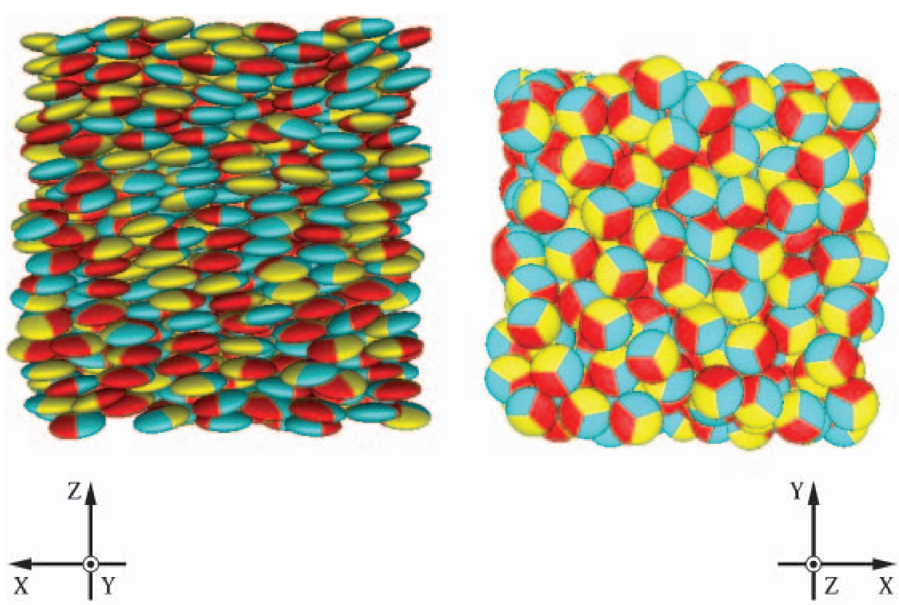

Figure 11. Snapshots of MC–NPT configurations (side and top views) of systems of $N=1000$ GB discs with three dipoles $\mu^*=0.6$ at $P^*=100$ and temperatures $T^*=4.0$ (phase N).

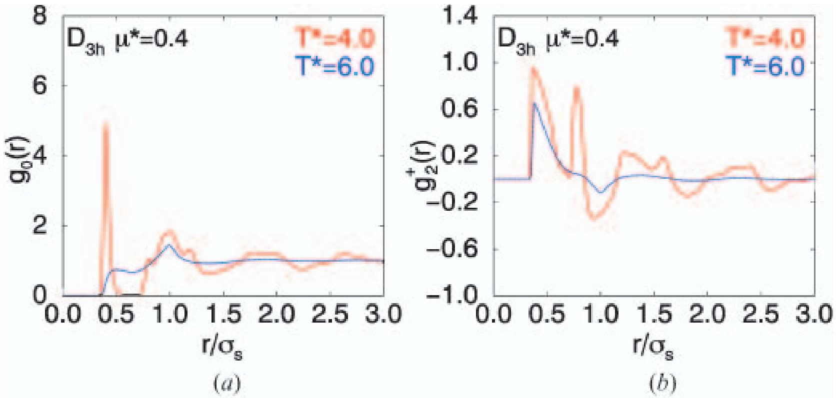

Figure 12. (*a*) Radial correlation function $g_0(r)$, (*b*) second rank anisotropy $g_2^+(r)$ for systems of $N=1000$ GB discs with three planar dipoles $\mu^*=0.4$ at $P^*=100$ and temperatures $T^*=4.0$ (phase C_h) and 6.0 (phase N).

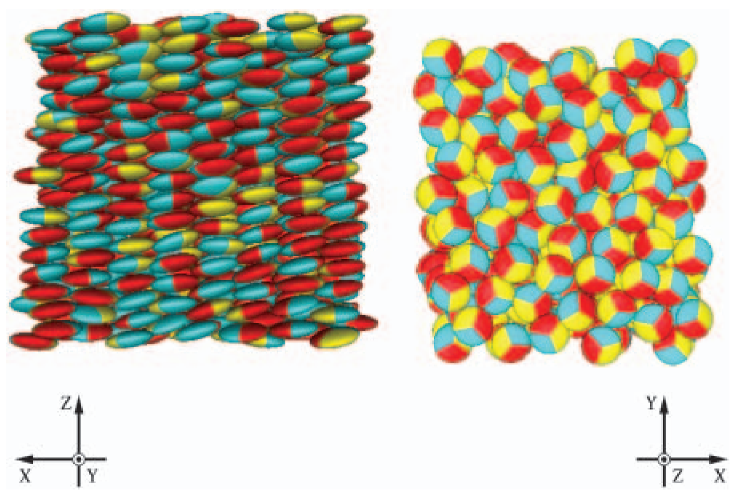

Figure 13. Snapshots of MC–NPT configurations (side and top views) of systems of $N=1000$ GB discs with three dipoles $\mu^*=0.4$ at $P^*=100$ and temperature $T^*=4.0$ (phase C_h).

the effect of their off-centre position, which allows interlocking, is quite different from that expected from a central quadrupole, as studied in [20, 21].

3.3. *Three dipoles* (D_{3h})

We now turn to the last case studied, where a third dipole is added to the discotic core as in figure 1, re-establishing an effective cylindrical symmetry since, at least from the point of view of second rank order parameters, a D_{3h} axis has the same effect as a $D_{\infty h}$ one. An immediate consequence is that $\langle R^2_{22}\rangle=0$ and no biaxial phase is present, see figures 8 (*b*) and 9 (*b*). It might be expected that the normal columnar phase is also re-established, but this is not necessarily so. In fact, the organization obtained depends on the strength of the dipole moments, as we have shown considering two cases: $\mu^*=0.4$ and $\mu^*=0.6$. Indeed, for $\mu^*=0.6$ the intermolecular dipole–dipole interaction leads to the disappearance of the columnar phase, and a highly ordered uniaxial nematic phase has been observed down to very low temperatures (see figure 8(*b*)). On the other hand, for the weaker dipole $\mu^*=0.4$, molecules are stacked in columns as for the previous dipoleless case and a short range order of the dipoles along the columns axis is observed (see figure 13).

To characterize the order in columnar stacks we calculate the angular distribution of $\theta_{i,j}$, the angle between the $\hat{\mathbf{x}}$ axis of a given molecule i, and the $\hat{\mathbf{x}}$ axis of a molecule j in the same column. We consider first ($j=i+1$) and second ($j=i+2$) neighbours, as well as molecules separated by distance equal to a half-stack. Note that for the D_{3h}, $\mu^*=0.4$ system the $\hat{\mathbf{x}}$ axis is geometrically correlated to the direction of the three dipoles, while for the dipoleless $D_{\infty h}$ system, the

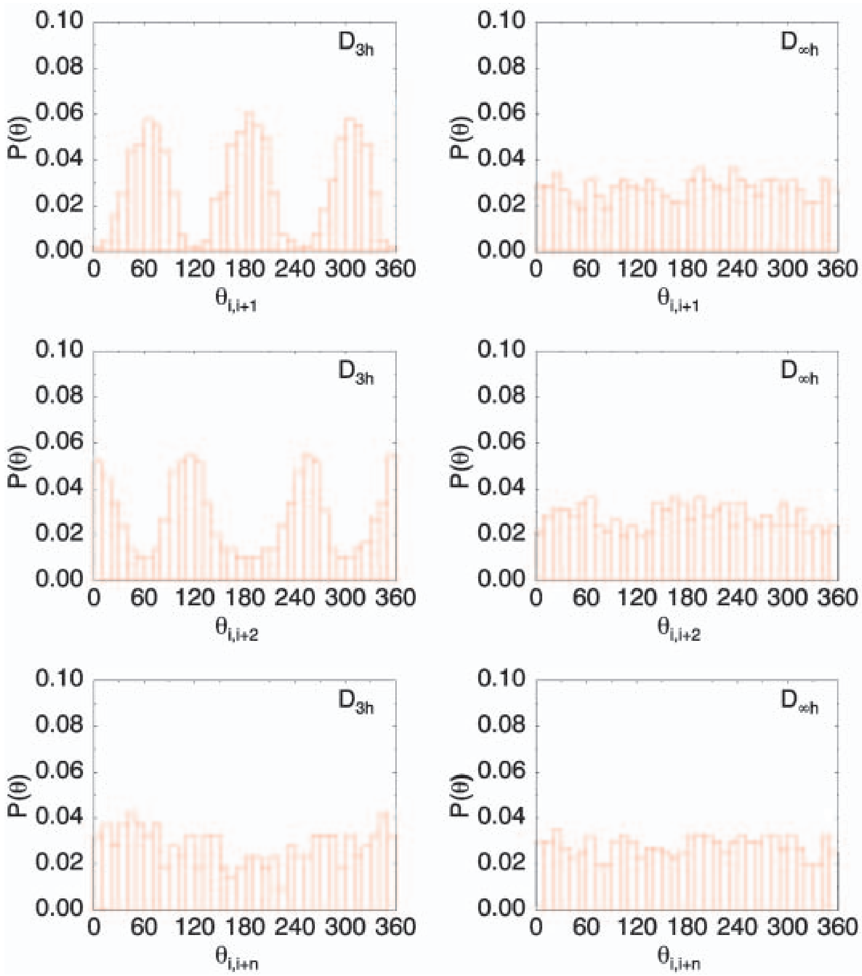

Figure 14. Distribution of angular twist $\theta_{i,j}$ along the columns for a system with three dipoles $\mu^*=0.4$ (left column, D_{3h}) and $\mu^*=0.0$ (right column, $D_{\infty h}$) at $T^*=4.0$. The three cases correspond to first ($\theta_{i,i+1}$) and second ($\theta_{i,i+2}$) neighbours, and to half column separation ($\theta_{i,i+n}$).

$\hat{\mathbf{x}}$ is an arbitrary fixed axis. An examination of figure 14 confirms that for the dipoleless system no preferred orientation about the axes of the columns in which they are stacked exists, and that all orientations $\theta_{i,j}$ are equivalent. Instead, in the D_{3h} case, dipolar interactions introduce an orientational correlation along the column axis; however, this angular correlation is short-ranged, and no long range transversal angular correlation lasting across the column has been found.

4. Conclusions

Our Monte Carlo simulations of Gay–Berne discs with local symmetrically placed dipoles have shown that the introduction of the dipolar interaction can have a profound influence on the phase organization, even for molecules that are overall apolar.

All the systems studied show a transition from isotropic to nematic and from nematic to a high ordered phase which is strictly dependent on dipole configuration and strength. Dipoleless Gay–Berne discotic particles form isotropic, nematic and hexagonal columnar mesophases, with weak correlations between columns. The columnar phase is destabilized by the addition of two or three strong lateral planar dipoles. For two and three planar dipoles $\mu^*=0.6$, in fact, no columnar structure is observed down to $T^*=3.0$; we find instead a strongly ordered nematic phase, while when dipoles are absent or with strength decreased, low temperature organizations correspond to columnar phases. We note that for the discs with two or three symmetrical dipoles the electrostatic energy is always negative with a magnitude which, for the dipole strength $\mu^*=0.6$, is at most 40% of the GB energy. The antiparallel association of the lateral dipoles gives rise to interdigitation between the different columns with the creation of less packed structures. In the two dipoles case, at low temperature, discotics are strongly interdigitated and show strong correlations in the plane perpendicular to the director and a large biaxiality.

No columnar phase is shown for the system with three relatively strong planar dipoles up to very low temperatures. Molecular stacks are completely interdigitated and no long range in-column transversal order is observed. However, changes of dipole strength have a significant effect on intra- and inter-columnar arrangements. In particular, on decreasing the strength of the three planar dipoles we again observe a columnar non-interdigitated phase, as in the apolar system.

We did not find evidence of chain structures, as found in many dipolar systems [22] because of the favourable head–tail disposition of point dipoles, but this is not surprising since our particles are non-polar overall and their dipoles are placed symmetrically and far apart (see figure 1), differently, for example, from rod-like particles with a transverse dipole [17, 22].

Acknowledgements

We wish to thank the University of Bologna, MIUR (PRIN Cristalli Liquidi), EU NAIMO Integrated Project (NMP4-CT-2004-500355), and INSTM for financial support.

References

[1] D. Guillon. *Structure and Bonding*, **95**, 41 (1999).
[2] S. Chandrasekhar. *Liquid Crystals*, 2nd Edn, Cambridge U.P., Cambridge (1992).
[3] S. Kumar. *Liq. Cryst.*, **31**, 1037 (2004).
[4] K. Praefcke, J.D. Holbrey. *J. inclusion Phenom. mol. recognition Chem.*, **24**, 19 (1996).
[5] H. Ringsdorf, R. Wüstefeld, E. Zerta, M. Ebert, J.H. Wendorff. *Angew. Chem. int. Ed.*, **28**, 914 (1989).
[6] J. Cornil, V. Lemaur, J.P. Calbert, J.L. Brèdas. *Adv. Mater.*, **14**, 726 (2002).
[7] A-J. Attias, C. Cavalli, B. Donnio, D. Guillon, P. Hapiot, J. Malthête. *Mol. Cryst. liq. Cryst.*, **415**, 169 (2004).
[8] O. Roussel, G. Kestemont, J. Tant, V. de Halleux, R. Gómez Aspe, J. Levin, A. Remacle, I. Raluca Gearba, D. Ivanov, M. Lehmann, Y. Geerts. *Mol. Cryst. liq. Cryst.*, **396**, 35 (2003).
[9] C. Zannoni. *J. Mater. Chem.*, **11**, 2637, and references therein (2001).
[10] R. Berardi, A.P.J. Emerson, C. Zannoni. *J. chem. Soc. Faraday Trans.*, **89**, 4069 (1993).
[11] A.P.J. Emerson, G.R. Luckhurst, S.G. Whatling. *Mol. Phys.*, **82**, 113 (1994).
[12] R. Berardi, S. Orlandi, C. Zannoni. *J. chem. Soc. Faraday Trans.*, **93**, 1493 (1997).
[13] R. Berardi, S. Orlandi, C. Zannoni. *PCCP*, **2**, 2933 (2000).
[14] J.A. Barker, R.O. Watts. *Mol. Phys.*, **26**, 789 (1973).
[15] A. Gil-Vilegas, S. McGrother, G. Jackson. *Mol. Phys.*, **92**, 723 (1997).
[16] M. Houssa, A. Oualid, L.F. Rull. *Mol. Phys.*, **94**, 439 (1998).
[17] R. Berardi, S. Orlandi, C. Zannoni. *Int. J. mod. Phys. C*, **10**, 477 (1999).
[18] F. Biscarini, C. Chiccoli, P. Pasini, F. Semeria, C. Zannoni. *Phys. Rev. Lett.*, **75**, 1803 (1995).
[19] A. Jaster. *Phys. Rev. E*, **59**, 2594 (1999).
[20] M.A. Bates, G.R. Luckhurst. *Liq. Cryst.*, **24**, 229 (1998).
[21] M.P. Neal, A.J. Parker. *Phys. Rev. E*, **63**, 011706 (2001).
[22] A. Gil-Villegas, S.C. McGrother, G. Jackson. *Chem. Phys. Lett.*, **269**, 441 (1997).

Appendix

Table 2. Results from MC–NPT simulations at pressure $P^*=100$ of a system of $N=1000$ GB discotic molecules for the Gay-Berne and dipolar energies per particle $\langle U_{ij}^{GB*} \rangle$ and $\langle U_{ij}^{d*} \rangle$, the orientational order parameter $\langle R_{00}^2 \rangle$ and the biaxial order parameter $\langle R_{22}^2 \rangle$ at temperatures T^* corresponding to isotropic (I), nematic (N_{bx}) and columnar (C_h) phases as indicated.

	T^*	Phase	$\langle U_{ij}^{GB*} \rangle$	$\langle U_{ij}^{d*} \rangle$	$\langle R_{00}^2 \rangle$	$\langle R_{22}^2 \rangle$
No dipoles	3.0	C_h	-37.9 ± 0.2		0.98 ± 0.01	—
	3.5	C_h	-36.0 ± 0.2		0.97 ± 0.01	—
	4.0	C_h	-33.9 ± 0.2	—	0.97 ± 0.01	—
	4.5	C_h	-31.6 ± 0.2	—	0.96 ± 0.01	—
	5.0	N	-25.1 ± 0.2	—	0.90 ± 0.01	—
	5.5	N	-18.1 ± 0.2	—	0.82 ± 0.01	—
	6.0	N	-14.9 ± 0.2	—	0.71 ± 0.01	—
	6.25	N	-12.8 ± 0.2		0.59 ± 0.01	—
	6.5	I	-10.3 ± 0.2	—	0.22 ± 0.01	—
	6.75	I	-9.6 ± 0.2	—	0.1 ± 0.01	—
	7.0	I	-8.9 ± 0.2	—	0.1 ± 0.01	—
	8.0	I	-7.5 ± 0.2	—	0.1 ± 0.01	—
Two dipoles	3.0	N_{bx}	-31.4 ± 0.2	-16.6 ± 0.2	0.98 ± 0.01	0.42 ± 0.01
	3.5	N_{bx}	-30.8 ± 0.2	-16.4 ± 0.2	0.98 ± 0.01	0.42 ± 0.01
	4.0	N_{bx}	-29.5 ± 0.2	-15.2 ± 0.2	0.98 ± 0.01	0.40 ± 0.01
	4.5	N_{bx}	-28.3 ± 0.2	-14.0 ± 0.2	0.97 ± 0.01	0.38 ± 0.01
	5.0	N	-19.1 ± 0.2	-4.6 ± 0.2	0.87 ± 0.01	—
	5.5	N	-17.0 ± 0.2	-3.8 ± 0.2	0.83 ± 0.01	—
	6.0	N	-14.9 ± 0.2	-3.2 ± 0.2	0.76 ± 0.01	—
	6.5	I	-12.1 ± 0.2	-2.5 ± 0.2	0.60 ± 0.01	—
	7.0	I	-9.1 ± 0.2	-1.8 ± 0.2	0.25 ± 0.01	—
	8.0	I	-7.2 ± 0.2	-1.3 ± 0.2	0.1 ± 0.01	—
Three	3.0	N	-27.4 ± 0.2	-22.8 ± 0.01	0.94 ± 0.01	—
dipoles	3.5	N	-26.4 ± 0.2	-21.2 ± 0.2	0.94 ± 0.01	—
$\mu^*=0.6$	4.0	N	-25.1 ± 0.2	-19.2 ± 0.2	0.94 ± 0.01	—
	4.5	N	-23.7 ± 0.2	-17.2 ± 0.2	0.92 ± 0.01	—
	5.0	N	-21.4 ± 0.2	-15.2 ± 0.2	0.88 ± 0.01	—
	5.5	N	-19.5 ± 0.2	-13.1 ± 0.2	0.87 ± 0.01	—
	6.0	N	-17.1 ± 0.2	-11.2 ± 0.2	0.82 ± 0.01	—
	6.5	I	-14.9 ± 0.2	-8.5 ± 0.2	0.76 ± 0.01	—
	7.0	I	-12.3 ± 0.2	-7.7 ± 0.2	0.61 ± 0.01	—
	7.5	I	-9.6 ± 0.2	-6.2 ± 0.2	0.32 ± 0.01	—
	8.0	I	-8.0 ± 0.2	-5.1 ± 0.2	0.1 ± 0.01	—
	9.0	I	-6.6 ± 0.2	-4.0 ± 0.2	0.1 ± 0.01	—
Three	3.0	C_h	-36.8 ± 0.2	-4.8 ± 0.1	0.98 ± 0.01	—
dipoles	3.5	C_h	-34.8 ± 0.2	-4.3 ± 0.1	0.97 ± 0.01	—
$\mu^*=0.4$	4.0	C_h	-32.4 ± 0.2	-3.8 ± 0.1	0.96 ± 0.01	—
	4.5	N	-22.0 ± 0.2	-3.2 ± 0.1	0.89 ± 0.01	—
	5.0	N	-20.4 ± 0.2	-2.9 ± 0.1	0.87 ± 0.01	—
	5.5	N	-18.0 ± 0.2	-2.4 ± 0.1	0.84 ± 0.01	—
	6.0	N	-15.2 ± 0.2	-1.9 ± 0.1	0.74 ± 0.01	—
	7.0	I	-9.1 ± 0.2	-1.2 ± 0.1	0.10 ± 0.01	—
	8.0	I	-7.5 ± 0.2	-0.9 ± 0.1	0.07 ± 0.01	—
	8.0	I	-6.5 ± 0.2	-0.7 ± 0.1	0.07 ± 0.01	—